

Coupled Navier Stokes- Molecular Dynamics Simulation using Iterative Operator-Splitting Methods

Jürgen Geiser¹ and Rene Steijl²

Humboldt Univeristät zu Berlin, D- Berlin, Germany
geiser@mathematik.hu-berlin.de

Abstract. In this paper, we contribute a multi-scale method based on an iterative operator splitting method, which takes into account the disparity of the macro- and microscopic scales. We couple Navier Stokes and Molecular Dynamics equations, while taken into account their underlying scales. Combining relaxation methods and averaging techniques we can optimize the computational effort.

The proposed method enables simulations in which the continuum flow aspects of the flow are described by the Navier-Stokes equations at time-scales appropriate for this level of modeling, while the viscous stresses within the Navier-Stokes equations are the result of Molecular Dynamics Simulations, with much smaller time-scales. The main benefit of the proposed method is that time-dependent flows can then be modeled with a computational work which is significantly smaller than when the complete flow would be modeled at molecular level, as a result of the different time-scales at the continuum and molecular levels, enabled by the application of the iterative operator-splitting method.

We discuss the convergence analysis to the splitting methods, see also [27].

Finally we present numerical results for the modified methods and applications to real-life flow problems.

Keywords Navier-Stokes equation, Molecular dynamics simulation, iterative operator-splitting method, coupling of micro- and macro-systems, dual-time stepping method.

AMS subject classifications: 65M06, 65L06, 47E05, 76D05, 74N15.

1 Introduction

We motivate our studying on combining multiple scale problems with time-decomposition methods. In the last years solving of multi-scale problems is a large topic. Important are solver methods to couple large scales, see [17] for lattice Boltzmann models, [2] for fluid dynamical problems. Numerically the delicate coupling of the continuous and discrete level is discussed in [23].

In our work we concentrate on optimizing the coupling process by a new method called iterative splitting. Iterative and relaxed splitting methods have their benefits in coupling time-scales, see [11] and [12]. For Navier-Stokes and Molecular Dynamics coupling different time-scale can be coupled by averaging and density ideas, see [2]. Here we present different algorithmic schemes to accelerate the solver process. We propose a new idea in considering splitting methods as simultaneous coupling schemes. The benefit in replacing the expensive MD simulations to a micro-scale viscous flux, which can be embedded into a fixed point iteration schemes is considered.

The paper is organized as follows. A mathematical model based on the coupled Navier Stokes and molecular dynamical equations is introduced in Section 2. The iterative splitting method for the nonlinear equation is given in Section 3. The computation of the molecular-level shear stress is given in Section 4. The implicit dual-time stepping method is discussed in Section 5. We introduce the numerical results in Section 6. Finally we discuss our future works in the area of splitting and decomposition methods for multi scale problems.

2 Mathematical Model

Our model equations are coming from fluid dynamics.

The macro-scale equation is given by the Navier-Stokes equation for incompressible continuum flow:

$$\rho \partial_t u + \rho(u \cdot \nabla)u - \mu \Delta u + \nabla p = \rho f, \text{ in } \Omega \times (0, T), \quad (1)$$

$$\nabla \cdot u = 0, \text{ in } \Omega \times (0, T), \quad (2)$$

$$u(0) = u_0, \text{ on } \Omega,$$

$$u = 0, \text{ on } \partial\Omega \times (0, T),$$

The unknown flow vector $u = u(x, t)$ is considered in $\Omega \times (0, T)$. In the above equations, ρ and p represent the fluid density and pressure, respectively. Here, μ represents the dynamic viscosity of the fluid. In the momentum equation, i.e. Equation (1), the term f on the right-hand side represents a volume source term. Equation (2) imposes the divergence-free constraint on the velocity field, which is consistent with the assumption of incompressible flow.

The micro-scopic equation is given by Newton's equation of motion for each individual molecule i for a sample of N molecules,

$$m_i \partial_{tt} x_i = F_i, i = 1, \dots, N, \quad (3)$$

here, the force F_i acting on each molecule is the result of the inter-molecular interaction of a molecule i with the neighbouring molecular within a finite interaction range. In the present work, we assume that the inter-particle forces are based on the well-known Lennard-Jones interaction potential[19], i.e. we are assuming the micro-scopic flow is that of a Lennard-Jones fluid, details of which are given in a later section.

The coupling between the macro-scale equation (1) and micro-scale equation (3) is assumed to take place through the exchange of the viscous stresses in the momentum equation (1). The underlying idea is to replace the viscous stresses based on the continuum Newtonian in Equation (1) with a viscous stress evaluated by Molecular Dynamics simulations of the micro-scale fluid with the velocity gradient at macro-scale level imposed on the micro-scale fluid, through the use of Lees-Edwards boundary conditions[18]. The molecular-level viscosity is evaluated using the Irving-Kirkwood relation[15].

The viscous stress contribution $\mu\Delta v$ in Equation (1) can be generalised for a non-Newtonian flow as $\partial\sigma_{ij}/\partial x_j$, using Einstein's summation. In the present work, this non-Newtonian viscous stress contribution is reformulated in the following form;

$$\partial\sigma_{ij}/\partial x_j = \mu_{apparent}\partial^2 v_i/\partial x_j^2 \quad (4)$$

where, the 'apparent' viscosity can be a general function of the imposed velocity gradients in each spatial direction, i.e. this expression can represent general non-continuum and non-Newtonian flow conditions. The viscous stresses in Equation (1) can now be replaced by molecular level viscous stresses by introducing a constant approximate viscosity μ_{approx} and take into account the deviation of the molecular-level viscous stresses from this approximate viscosity through a volumetric source term.

So, finally, we obtain the coupled multi-scale equations:

$$\begin{aligned} \rho\partial_t v + \rho(v \cdot \nabla)v - \mu_{approx}\Delta v + \nabla p &= f, \text{ in } \Omega \times (0, T), \\ f_i &= \partial\sigma_{ij}/\partial x_j|_{molecular} - \mu_{approx}\Delta v_i \end{aligned} \quad (5)$$

where Einstein's summation is used for the volumetric source term f , which accounts for the deviation of the viscous stresses evaluated at molecular-level from the approximate Newtonian relation $\mu_{approx}\Delta v$. The molecular-level viscous stresses can be further reformulated using the 'apparent' viscosity, as demonstrated in Equation (4).

3 Iterative splitting method

The following algorithm is based on the iteration with fixed splitting discretization step-size τ . The splitting scheme can be formulated as a predictor corrector scheme or three steps method. On the time interval $[t^n, t^{n+1}]$ we solve the fol-

lowing sub-problems consecutively for $i = 1, 2, \dots, M$.

$$\frac{\partial c_i(t)}{\partial t} = Ac_i(t) + Bp_{i-1}(t), \text{ with } c_i(t^n) = c^n \quad (6)$$

$$i = 1, 2, \dots, j, \quad (7)$$

$$Bp_{i+1}(t) = f(c_i), \quad (8)$$

$$i = j + 1, j + 2, \dots, m, \quad (9)$$

$$\frac{\partial c_{i+2}(t)}{\partial t} = Ac_i(t) + Bp_{i+1}(t), \text{ with } c_{i+2}(t^n) = c^n \quad (10)$$

$$i = m + 1, m + 2, \dots, M, \quad (11)$$

where we assume the operator A has a large time scale and B has a small time scale.

Here we decouple the different time-scales and stabilise the scheme with averaging functions f .

Theorem 1. *Let us consider the abstract Cauchy problem in a Banach space \mathbf{X}*

$$\partial_t c(t) = Ac(t) + Bp(t), \quad 0 < t \leq T, \quad (12)$$

$$Bp = f(c), \quad (13)$$

$$c(0) = c_0, \quad (14)$$

where $A, B, A + B : \mathbf{X} \rightarrow \mathbf{X}$ are given linear operators being generators of the C_0 -semigroup and $c_0 \in \mathbf{X}$ is a given element. Then the iteration process (6)–(8) is convergent and the rate of the convergence is of higher order.

The proof could be found in [11].

More detailed, we can consider the iterative operator splitting method as a waveform relaxation form with multiple steps. This help to understand the algorithmic implementation of the schemes, see applications in [20].

So let us consider the following scheme :

Waveform-Relaxation Method:

$$\frac{du_i}{dt} = Pu_i + Qu_{i-1} + f, \quad (15)$$

$$u_i(t^n) = u(t^n), \quad (16)$$

where $A = P + Q$, e.g. P is the diagonal part of A (Jacobi-method).

Here the splitting method is done abstract with respect to the matrix A . The method considered an effective solver method with respect to the underlying matrices.

Iterative Operator Splitting Method:

$$\frac{du_i}{dt} = Pu_i + Qu_{i-1} + f, \quad (17)$$

$$u_i(t^n) = u(t^n), \quad (18)$$

$$\frac{du_{i+1}}{dt} = Pu_i + Qu_{i+1} + f, \quad (19)$$

$$u_{i+1}(t^n) = u(t^n), \quad (20)$$

where P, Q are matrices given by spatial discretisation, e.g. P is the convection part of Q the diffusion part.

But we can also do an abstract decomposition, take into account $A = P + Q$, where P is the matrix with small eigenvalues and Q is the matrix with large eigenvalues.

4 Molecular-Level Shear Stress Computation

In the present work, the micro-scopic model is given by the Newton equations for the motion of individual molecules, for which the well-known Molecular Dynamics (MD) method[1] is used. The MD method simulates the dynamics of a system of N interacting molecules by temporal integration of the Newton's equations of motion, for which the velocity Verlet algorithm[25], which is second-order accurate in time, is used,

$$\begin{aligned} \underline{x}_i^{(n+1)} &= \underline{x}_i^{(n)} + \delta t \underline{v}_i^{(n)} - \frac{\delta t^2}{2m_i} \nabla U_i^{(n)} & i = 1, \dots, N \\ \underline{v}_i^{(n+1)} &= \underline{v}_i^{(n)} + \frac{\delta t}{2m_i} \nabla U_i^{(n)} & i = 1, \dots, N \end{aligned} \quad (21)$$

In the present work, the Lennard-Jones fluid is used as a model, i.e. an atomic medium with an inter-particle potential given by:

$$U_{LJ}(r_{ij}) = 4\epsilon_{ij} \left[\left(\frac{\sigma_{ij}}{r_{ij}} \right)^{12} - \left(\frac{\sigma_{ij}}{r_{ij}} \right)^6 \right] \quad (22)$$

where r_{ij} is the distance between particles i and j , ϵ_{ij} is the depth of the potential well and σ_{ij} is the (finite) distance at which the inter-particle potential is zero. The Lennard-Jones potential combines strong repulsion at short distances with weak attraction at longer distances. In the above equation, σ_i as well as ϵ_i are assumed identical for $i = 1, \dots, N$. Furthermore, a cut-off distance r_c is defined.

To model hydrodynamics using the MD method, the following steps are typically employed. First, a number of micro-scopic domains are initialised with randomly-placed particles at the number density consistent with the prescribed fluid density. Secondly, using an appropriate time-integration method, coupled with a thermostat to control the temperature, the micro-scopic solutions are integrated sufficiently long to reach an equilibrium solution at the prescribed density and temperature. Following this initial equilibration phase, the micro-scopic

equations are further integrated in time. In the phase, the particle positions and velocity are used to compute averaging in space and time, as well as, ensemble averaging when multiple micro-scopic solutions are considered.

Figure 1 presents the results from a large number of Molecular Dynamics simulations for a cubic domain of dimension 12σ with a 1382 particles, i.e. the density in Lennard-Jones units is 0.8. For a range of velocity gradients imposed linearly on this domain, the shear stresses are presented. Results are compared for ensemble averaging over 4, 8 and 16 independent realisations and for sampling durations of 100 and 200 τ . The time-steps in the MD simulations are 0.001 τ .

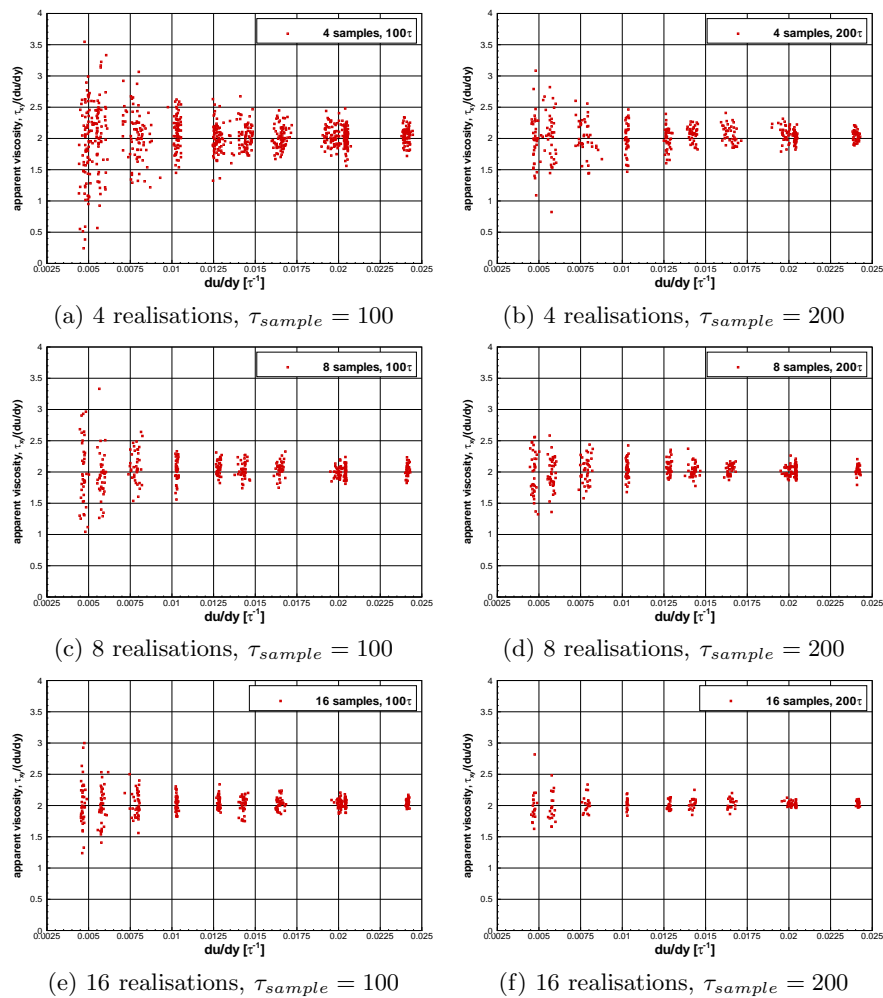


Fig. 1. Effect of number of independent realisations and sampling duration on the statistical scatter in the predicted apparent viscosity. Lennard-Jones fluid at $0.80\sigma^{-3}$ and $T = 1.50$.

5 Implicit dual-time stepping method for time-dependent flows

We start with a first example to use the stable first order splitting as a pre-step method and then start with the higher order iterative method.

5.1 Governing equations for macro-scale and micro-scale problems

The Navier-Stokes equations written in integral form for a domain fixed in time, read

$$\frac{d}{dt} \int_{V(t)} \mathbf{w} dV + \int_{\partial V(t)} (\mathbf{F}(\mathbf{w}) - \mathbf{F}_v(\mathbf{w})) \mathbf{n} dS = \mathbf{S}. \quad (23)$$

The above forms a system of conservation laws for any fixed control volume V with boundary ∂V and outward unit normal \mathbf{n} . The vector of conserved variables is denoted by $\mathbf{w} = [\rho, \rho u, \rho v, \rho w, \rho E]^T$, where ρ is the density, u, v, w are the Cartesian velocity components and E is the total internal energy per unit mass. \mathbf{F} and \mathbf{F}_v are the inviscid and viscous flux, respectively. In the absence of volume forces and in an inertial frame of reference the source term $\mathbf{S} = 0$.

Assuming that the x -direction is the homogeneous direction, the y direction is the cross-flow direction, as well as, that the flow is incompressible with vanishing velocity components in the y and z directions, the governing equation can then be written as,

$$\begin{aligned} \rho \partial u / \partial t - \mu_{approx} \partial^2 u / \partial x^2 + \partial p / \partial x &= f, \\ f &= \partial \sigma_{xy} / \partial x - \mu_{approx} \partial^2 u / \partial x^2 \end{aligned} \quad (24)$$

using the multi-scale equation (5).

Equations (23) are discretised using a cell-centred finite volume approach on structured multi-block grids which leads to a set of ordinary differential equations in time of the form

$$\frac{\partial}{\partial t} (\mathbf{w}_{i,j,k} V_{i,j,k}) = -\mathbf{R}_{i,j,k}(\mathbf{w}_{i,j,k}) \quad (25)$$

where \mathbf{w} and \mathbf{R} are the vectors of cell variables and residuals, respectively. Here, i, j, k are the cells indices in each block and $V_{i,j,k}$ is the cell volume.

In the present work, the flow problems considered lead to a reduction of the full Navier-Stokes equations to a set of equations for the velocity field components. Hence, the vector \mathbf{w} in this work only involves the Cartesian velocity components, while \mathbf{R} represents the residuals of the three moment equations.

Boundary conditions are imposed by using two layers of halo cells around each grid sub-domain. Zero-slip conditions at solid walls are imposed by extrapolating halo cell values such that the velocity at the wall vanishes.

5.2 Dual-time stepping method

For time-accurate simulations, temporal integration is performed using an implicit dual-time stepping method. Following the pseudo-time formulation [?], the updated mean flow solution is calculated by solving the steady state problems

$$\mathbf{R}_{i,j,k}^* = V_{i,j,k} \frac{3\mathbf{w}_{i,j,k}^{n+1} - 4\mathbf{w}_{i,j,k}^n + \mathbf{w}_{i,j,k}^{n-1}}{2\Delta t} + \mathbf{R}_{i,j,k}(\mathbf{w}_{i,j,k}^{n+1}) = 0 \quad (26)$$

Equation (26) represents a nonlinear system of equations for the full set of Navier-Stokes equations. However, for the reduced system of equations resulting from the homogeneity and periodicity assumptions, presented in Equation (24), the system of equations is actually linear. This system is solved by introducing an iteration through *pseudo time* τ to the steady state, as given by

$$\frac{\mathbf{w}_{i,j,k}^{n+1,m+1} - \mathbf{w}_{i,j,k}^{n+1,m}}{\Delta\tau} + \frac{3\mathbf{w}_{i,j,k}^{n+1,m} - 4\mathbf{w}_{i,j,k}^n + \mathbf{w}_{i,j,k}^{n-1}}{2\Delta t} + \frac{\mathbf{R}_{i,j,k}(\mathbf{w}_{i,j,k}^{n+1,m})}{V_{i,j,k}^{n+1}} = 0 \quad (27)$$

where the m -th pseudo-time iterate at real time step $n+1$ is denoted by $\mathbf{w}^{n+1,m}$ and the cell volumes are constant during the pseudo-time iteration. The unknown $\mathbf{w}_{i,j,k}^{n+1}$ is obtained when first term in in Equation (26) converges to a specified tolerance. An implicit scheme is used for the pseudo-time integration. The flux residual $\mathbf{R}_{i,j,k}(\mathbf{w}_{i,j,k}^{n+1})$ is linearised as

$$\begin{aligned} \mathbf{R}_{i,j,k}(\mathbf{w}^{n+1}) &= \mathbf{R}_{i,j,k}(\mathbf{w}_{i,j,k}^n) + \frac{\partial \mathbf{R}_{i,j,k}(\mathbf{w}_{i,j,k}^n)}{\partial t} \Delta t + O(\Delta t^2) \\ &\approx \mathbf{R}_{i,j,k}^n(\mathbf{w}_{i,j,k}^n) + \frac{\partial \mathbf{R}_{i,j,k}^n}{\partial \mathbf{w}_{i,j,k}^n} (\mathbf{w}_{i,j,k}^{n+1} - \mathbf{w}_{i,j,k}^n) \end{aligned} \quad (28)$$

Using this linearisation in pseudo-time, Equation (27) becomes a sparse system of linear equations. For the solution of this system, the Conjugate Gradient method with a simple Jacobi pre-conditioner is used.

5.3 Time-dependent channel flow simulation

In this section, the flow in a square channel is considered. The mean flow direction is the x -direction, while the channel lower and upper walls are placed at $z = 0\sigma$ and $z = 40\sigma$, respectively. The flow is assumed constant in y -direction. The considered domain is 40σ long in all three coordinate direction. Although the flow is two-dimensional, a three-dimensional solution method is used here, hence the use of the constant y -direction. A finite-volume discretisation method is used with a uniform mesh with 10 cells in both x - and y -directions, while a stretched mesh with 20 cells is used in the z -direction. The time-dependent problem starts from a steady flow established by a constant pressure gradient $dp/dx = -0.005$. From time $t = 100$ to $t = 500$ this pressure gradient is then linearly increased to $dp/dx = -0.010$. The time-step used in the finite-volume

method is $dt = 2$ (macro-scale time units). The Molecular Dynamics method is used in this example to evaluate the viscous stresses on the first 4 cells face near both domain walls, i.e. the cell face on the solid wall and the first three faces away from the wall. Due to the homogeneity and periodicity of the flow, these 4 micro-scale solutions are similarly used for the whole $x - y$ planes for the near-wall cell layers. Due to the symmetry of the problem, these 'micro-scale' viscous are re-used for both lower and upper domain walls. The remaining cell faces use a Newtonian fluid assumption for the viscous flux formulation, with the viscosity of the medium is assumed constant at $\mu = 2.0$.

For the idealised case in which all cell faces use Newtonian viscous stresses, the solution of this flow problem is shown as the solid black line in Figure 2(a), where the velocity in the centre of the domain is plotted versus time.

For the Lennard-Jones fluid considered in the Molecular Dynamics method, the density is assumed to be $0.80\sigma^{-3}$, while the temperature is $T = 1.50$. For these conditions, the Lennard-Jones fluid has a viscosity of around 2.03, i.e. very close to the assumed constant value in the Newtonian fluid part of the computational domain. As discussed previously, the viscous stresses as function of the imposed velocity gradients are computed using the Lees-Edwards boundary conditions. In the Molecular Dynamics simulations, ensemble as well as temporal averaging is employed. Typically, 4 or 8 independent realisations for each shear-rate are constructed, which are then sampled through a sampling duration of typically 100 Lennard-Jones time units. For the MD time-step here, i.e. 0.001τ , this involves 100,000 MD time steps.

5.4 Approximation of statistical scatter in micro-scale problems

In the present work, time-splitting methods are designed which can be regarded as extensions to the the dual-time stepping method described in the previous sections. To facilitate this algorithm design process, it is important to reduce the computational cost of the present channel flow simulations, since in this process many different parameters will have to be evaluated. The most time-consuming part of the algorithms is the present work, is the micro-scale Molecular Dynamics shear stress evaluations. To reduce computational cost in this investigation, the computationally expensive MD simulations are actually replaced by a modelled micro-scale viscous flux. The aim of these model micro-scale problems is to provide an equivalent of the micro-scale MD viscous stresses for a given velocity gradient with a statistical scatter sampled from a random distribution. The amplitude of the random statistical scatter in the predicted micro-scale viscous stresses is derived from the actual MD data from the simulations of the previous section. Figure 5 and 6 show the predicted apparent viscosity from the 24 time-steps at which a full MD viscous stress evaluation was conducted for the 4 cell faces nearest to the domain walls. The predicted apparent viscosity are plotted versus the sampling duration. Also shown are the average, as well as, the L_2 , L_4 and L_6 norms of deviation from this average. Based on this data, an approximate statistical scatter as function of the sampling duration is derived based on the L_6 norm, as shown in the figures.

6 Numerical Experiments: Splitting methods for coupled micro-macro system of equations

In this section, three time-integration methods derived from the implicit dual-time stepping method are derived and evaluated for the time-dependent channel flow example problem.

6.1 Method 1: fixed-interval micro-scale evaluations

In this first example, the coupling with the Molecular Dynamics method takes place by introducing a correction to the Newtonian shear stresses for the cell faces with an associated micro-scale MD shear stress evaluation, as presented in Equation (24). In this method, the following steps are used:

- for time step $j = 100$, the solution is marched forward in time using the Newtonian shear stresses evaluation employed throughout the domain
- at time step 20, 40, 60, 80 and 100, a micro-scale MD problems are constructed for the 4 cell faces nearest to the domain walls. For each cell face, 4 independent realisations are created, while the viscous stresses are sampled over 100τ after an initial equilibration stage of 50τ .
- for time steps $j > 100$, the viscous fluxes in the 4 cell faces nearest to the domain walls are corrected using an apparent viscosity derived from averaging over the last 5 MD evaluations for each cell face
- every 20 time steps, another set of micro-scale MD problems are constructed based on the current cell face velocity gradient, and following a new set of MD viscous stress evaluations, the 'averaged apparent' viscosity is updated

The above method is a simple method to take into account the shear-rate dependence of the apparent viscosity, while greatly reducing the computational overhead compared to a full set of MD shear stress evaluations computed for each macro-scale time step. However, for rapidly changing macro-scale velocity gradient, using the 'running' average of the latest MD predictions with a number of previous evaluations, introduced a potential time-lag in incorporating the shear-rate dependence of the apparent viscosity.

The method can be summarized as follows:

Algorithm 2 *On a uniform time grid with $t^n = t_0 + n\Delta t$, $n = 0, \dots, N$, (where N is given), the discretized coupled macro- and micro-scale equations are integrated in time from time level n to $n + 1$ using the following scheme:*

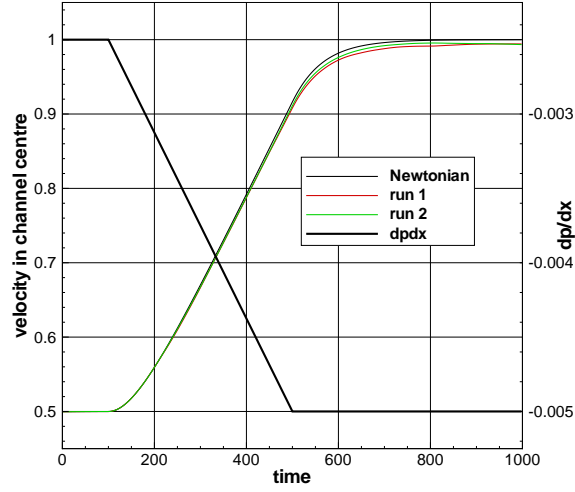
- 1) initialize averaged apparent viscosity $\mu_{ave} = \mu_{approx}$
- 2) if $n < 100$ and n is multiple of $n_{interval}$ go to 3) else go to 4)
- 3) dual-time step update based on fixed μ_{ave}
 - i) for the cell faces with micro-scale fluxes, compute the velocity gradients
 - ii) construct the viscous flux corrections f_i using updated apparent viscosity
 - iii) perform dual-time step update using n_{Newton} relaxation steps

- 4) *dual-time step update based on updated μ_{ave}*
- i) for the cell faces with micro-scale fluxes, compute the velocity gradients*
 - ii) initialize the Molecular-Dynamics micro-scale problems with the imposed velocity gradients from the finite-volume cell faces and integrate these through the initial equilibration phase (e.g. $t_{equi} = 50\tau$)*
 - iii) integrate micro-scale problems in time through t_{sample} micro-scale time and average apparent viscosity in time and ensemble average over $n_{ensemble}$ independent realizations*
 - iv) compute new μ_{ave} as average over last n_{window} (including present) Molecular Dynamics solutions*
 - v) contract the viscous flux corrections f_i using updated apparent viscosity*
 - vi) perform dual-time step update using n_{Newton} relaxation steps*
- if $n < N$ go to 1)*

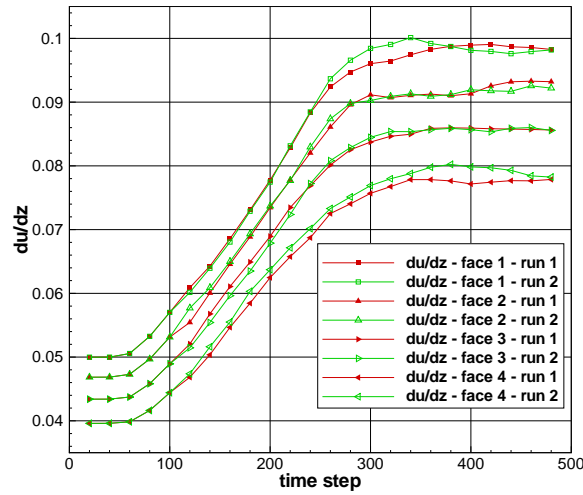
Figure 2 presents the results for the velocity predicted with the above method from two independent realisations. Compared to the idealised case with Newtonian fluxes throughout the domain, the use of MD micro-scale fluxes leads to a small reduction in the cell centre velocity, since the apparent viscosity predicted by the MD simulations is slightly higher than the constant viscosity used in the remainder of the domain. Also, using the averaging over 5 evaluations, the statistical scatter in the MD micro-scale fluxes only leads to modest fluctuations in the macro-scale velocity field compared to the fully Newtonian case.

The predicted apparent viscosity and the resulting 'running averages' are presented in Figure 3, clearly showing the significant reduction of the statistical scatter in the MD data when such an averaging is used in addition to the already used temporal and ensemble averaging.

The present dual-time stepping method solves a 'quasi-steady' problem at each time step. For each of these 'quasi-steady' problems, an implicit solution method is used based on an under-relaxed Newtonian relaxation process. The convergence of this implicit system for a number of time-steps is presented in Figure 4. In the examples shown, 25 'pseudo-steps' are used, leading to a reduction of the maximum norm of the residual (which now includes the 'unsteady' flow contribution) of at least 6 orders of magnitude. When this residual norm is reduced to machine precision, the only discretisation errors due to the time discretisation are those due to the truncation errors in the employed implicit 3-point stencil. With a reduction of the residual norm of 6 or 7 order of magnitude it can be expected that the additional contributions are much smaller than the truncation errors in the implicit 3-point stencil.

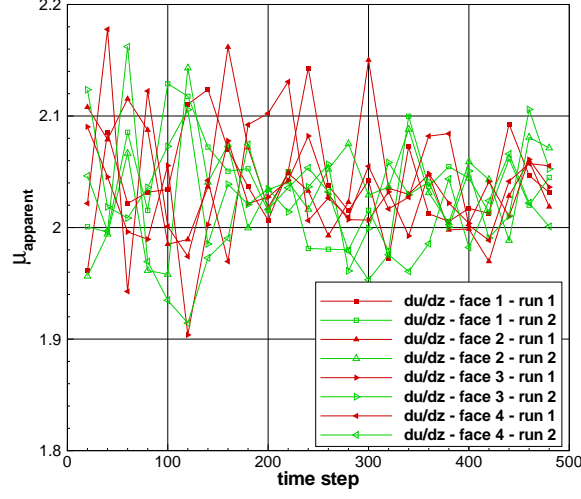


(a) Velocity in channel centre

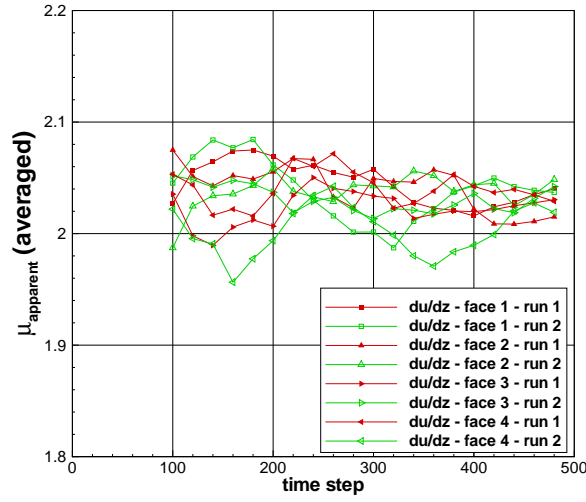


(b) Velocity gradients near walls

Fig. 2. Channel flow with time-dependent pressure gradient. Dual-time stepping method with averaging of apparent viscosity. Finite-volume discretization method with Molecular Dynamics viscous fluxes on first 4 cells near lower and upper walls. Lennard-Jones fluid at $0.80\sigma^{-3}$ and $T = 1.50$. MD data averaged over 4 realisations, $\tau_{sample} = 100$.

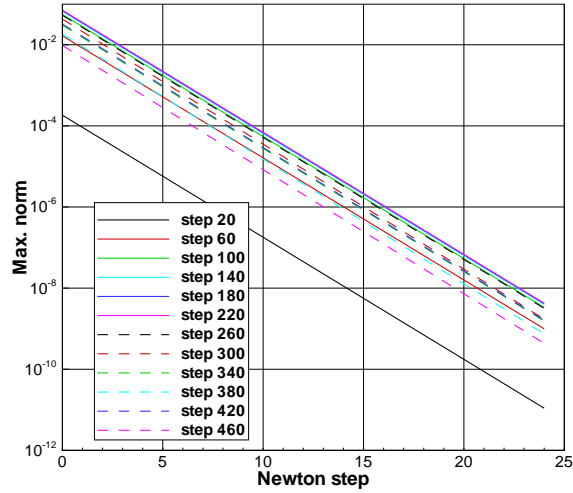


(a) apparent viscosity

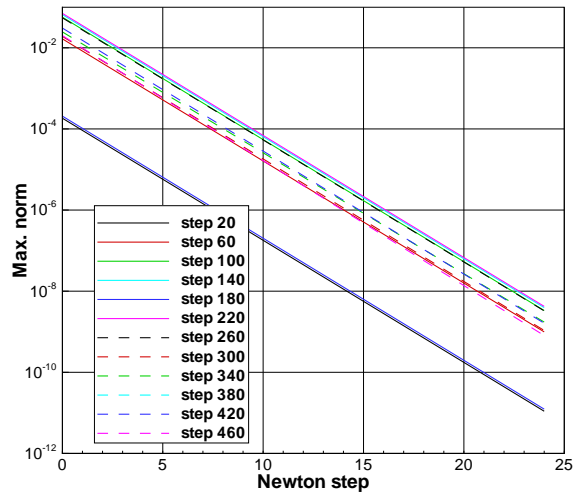


(b) averaged apparent viscosity

Fig. 3. Channel flow with time-dependent pressure gradient. Dual-time stepping method with averaging of apparent viscosity. Finite-volume discretization method with Molecular Dynamics viscous fluxes on first 4 cells near lower and upper walls. Lennard-Jones fluid at $0.80\sigma^{-3}$ and $T = 1.50$. MD data averaged over 4 realisations, $\tau_{\text{sample}} = 100$.

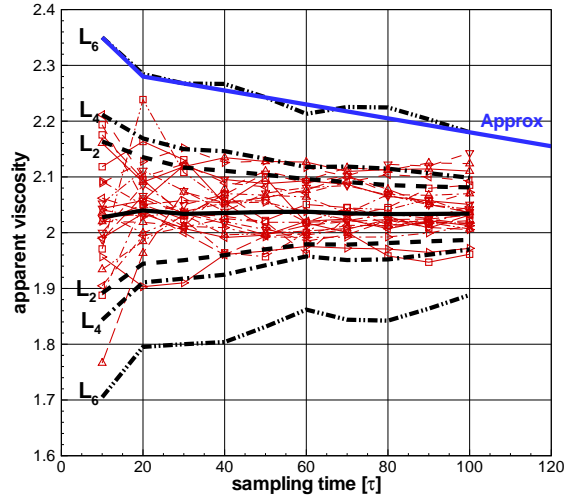


(a) realisation 1

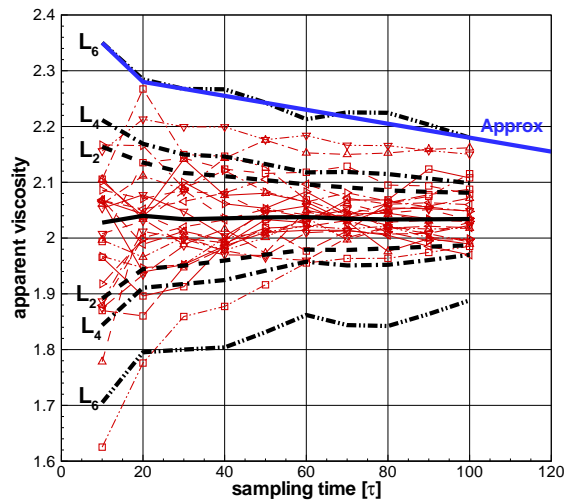


(b) realisation 2

Fig. 4. Channel flow with time-dependent pressure gradient. Dual-time stepping method with averaging of apparent viscosity. Convergence of 'inner-loop' in dual-time step method. Channel flow with time-dependent pressure gradient. Lennard-Jones fluid at $0.80\sigma^{-3}$ and $T = 1.50$. MD data averaged over 4 realisations, $\tau_{sample} = 100$.

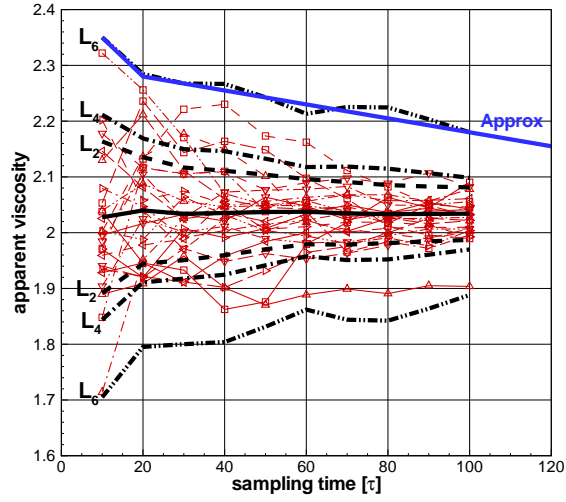


(a) face 1

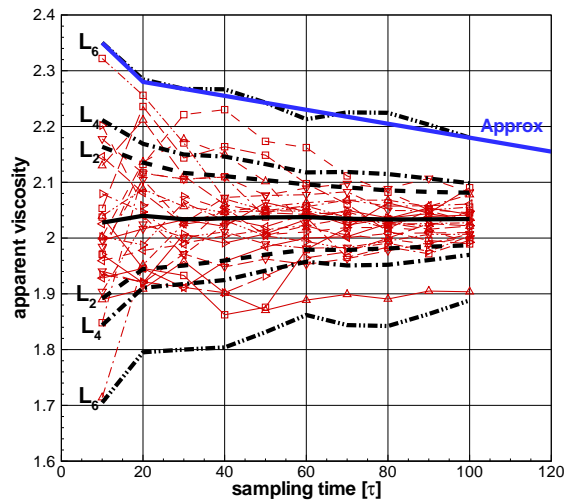


(b) face 2

Fig. 5. Convergence of predicted apparent viscosities in 4 cells faces as function of sampling time. Lennard-Jones fluid at $0.80\sigma^{-3}$ and $T = 1.50$. MD data averaged over 4 realisations, $10 \leq \tau_{sample} \leq 100$.



(a) face 3



(b) face 4

Fig. 6. Convergence of predicted apparent viscosities in 4 cells faces as function of sampling time. Lennard-Jones fluid at $0.80\sigma^{-3}$ and $T = 1.50$. MD data averaged over 4 realisations, $10 \leq \tau_{sample} \leq 100$.

6.2 Method 2: dual-time stepping method with fixed-point iteration

In this second method, the coupling with the Molecular Dynamics method takes place by introducing a correction to the Newtonian shear stresses for the cell faces with an associated micro-scale MD shear stress evaluation, as presented in Equation (24). In this method, the following steps are used:

- for time step $j = 100$, the solution is marched forward in time using the Newtonian shear stresses evaluation employed throughout the domain
- for time steps $j > 100$, the viscous fluxes in the 4 cell faces nearest to the domain walls are corrected data derived from Molecular Dynamics micro-scale problems. For each cell face, 4 independent realisations are created, followed by an initial equilibration stage of 50τ and an initial sampling time of 10τ . Using the MD predictions, the dual-time stepping method is used to create the velocity field for fixed-point iteration 0,
- for fixed-point iteration $1, \dots, n$, the MD micro-scale solutions are integrated for a further 10τ sampling durations. With the updated MD predictions, the dual-time stepping method is used to create the velocity field for this fixed-point iteration

In the above method, the number of fixed-point iterations is assumed to be constant number. The method can be summarized as follows:

Algorithm 3 *On a uniform time grid with $t^n = t_0 + n\Delta t$, $n = 0, \dots, N$, (where N is given), the discretized coupled macro- and micro-scale equations are integrated in time from time level n to $n + 1$ using the following scheme:*

- 1) *For the cell faces with micro-scale fluxes, compute the velocity gradients*
- 2) *Initialize the Molecular-Dynamics micro-scale problems with the imposed velocity gradients from the finite-volume cell faces and integrate these through the initial equilibration phase (e.g. $t_{equi} = 50\tau$)*
- 3) *Dual-time step with fixed-point iteration. Perform the following steps:*
 - i) set fixed point counter $iter = 0$*
 - ii) integrate micro-scale problems in time through an additional 10τ and sample apparent viscosity through total micro-scale sampling time and ensemble average over $n_{ensemble}$ independent realizations*
 - iii) construct the viscous flux corrections f_i using updated apparent viscosity*
 - iv) perform dual-time step update using n_{Newton} relaxation steps*
 - v) if $iter < n_{fp}$, increment $iter$ and go to i)*

if $n < N$ go to 1)

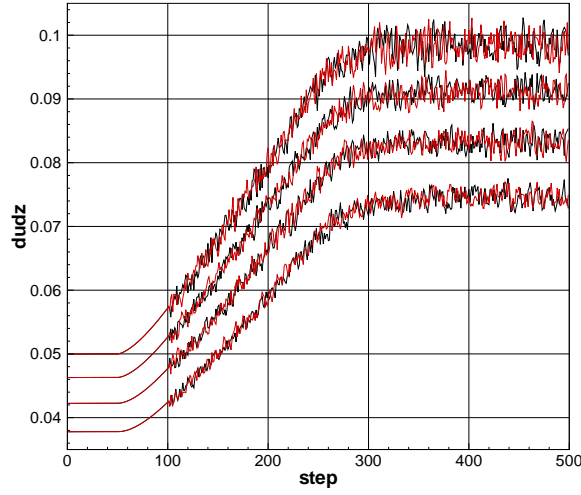
In the next section, a more adaptive method is devised which adjusts the number of fixed-point iterations with an appropriate error norm on both viscous flux corrections and velocity field updates.

In this section, the expensive MD simulations are replaced with a modelled micro-scale scale prediction for the apparent viscosity,

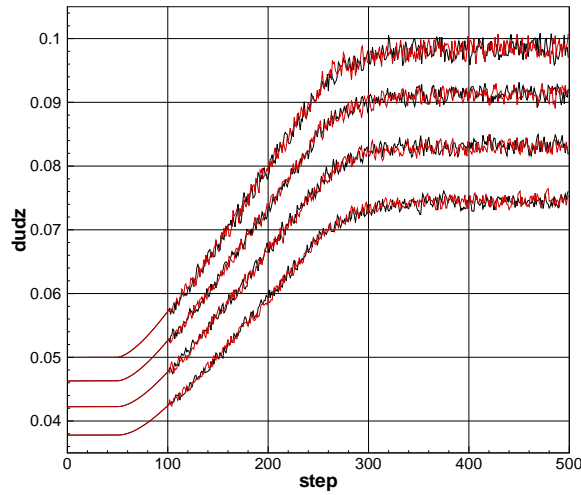
$$\mu_{apparent} = 2.03 + \mu_{scatter}(t_{sampling})rand() \quad (29)$$

where the statistical scatter amplitude is shown in Figure 5 and 6, with a linear continuation to zero scatter for sampling times exceeding 200τ . Clearly, this is an idealised situation, but allows an initial assessment of the time-splitting methods developed in the present work.

In the examples presented here, 10 fixed point iterations lead to a statistical scatter in the predicted micro-scale viscosities of similar magnitude as the full MD sampling over 100τ used in the previous section. For 20 fixed point iterations and more, the statistical scatter is removed completely, leading to a constant viscous flux correction due to the fact that the modelled value of 2.03 is slightly higher than the constant value used in the Newtonian shear stress evaluation.



(a) Velocity gradients near walls - 10 fixed-point inner iterations



(b) Velocity gradients near walls - 15 fixed-point inner iterations

Fig. 7. Channel flow with time-dependent pressure gradient. Dual-time stepping method with fixed-point iteration in MD sampling of apparent viscosity. Finite-volume discretization method with approximated statistical scatter of Molecular Dynamics viscous fluxes as function of sampling duration on first 4 cells near lower and upper walls.

6.3 Method 3: adaptive fixed-point iteration

The final method presented here is based on an adaptive splitting approach, i.e. one which truncates the fixed-point iteration whenever the viscous flux corrections and/or the velocity field updates relative to the previous fixed point iterations fall below a certain threshold. In this respect, it is a modified version of the algorithm used in the previous section. The method can be summarized as follows:

Algorithm 4 *On a uniform time grid with $t^n = t_0 + n\Delta t$, $n = 0, \dots, N$, (where N is given), the discretized coupled macro- and micro-scale equations are integrated in time from time level n to $n + 1$ using the following adaptive scheme:*

- 1) For the cell faces with micro-scale fluxes, compute the velocity gradients
- 2) Velocity gradient criterion: $\max \left(\left| \left(\frac{\partial u_i}{\partial x_j} \right)_{micro}^n - \left(\frac{\partial u_i}{\partial x_j} \right)_{micro}^{last} \right| \right) > crit_{grad}$, $crit_{grad} \in \mathbb{R}^+$. If criterion is satisfied goto 3) else 4)
- 3) Dual-time step with fixed-point iteration. Perform the following steps:
 - i) Using the last estimate of the micro-scale apparent viscosity, compute an estimate of the updated velocity field at the present time step using dual-time step update.
 - ii) Compute the velocity normalization factor as: $u_{norm} = \max(\tilde{u}_i(t^{n+1} - u_i(t^n))$, where \tilde{u} denotes the estimated velocity from step i)
 - iii) Compute viscous flux correction normalization as: $f_{norm} = \max(\tilde{f}_i(t^{n+1}))$, with \tilde{f} the viscous flux correction based on the last apparent viscosity computation
 - iv) Store micro-scale velocity gradients: $\left(\frac{\partial u_i}{\partial x_j} \right)_{micro}^{last} = \left(\frac{\partial u_i}{\partial x_j} \right)_{micro}^n$
 - v) Initialize the Molecular-Dynamics micro-scale problems with the imposed velocity gradients from the finite-volume cell faces and integrate these through the initial equilibration phase (e.g. $t_{equi} = 50\tau$)
 - vi) Fixed-point iteration:
 - a) integrate micro-scale problems in time through an additional 10τ and sample apparent viscosity through total micro-scale sampling time and ensemble average over $n_{ensemble}$ independent realizations
 - b) contract the viscous flux corrections f_i using updated apparent viscosity
 - c) perform dual-time step update using n_{Newton} relaxation steps
 - d) check convergence of fixed-point iteration using the stop criteria: $|u_i(t^{n+1}) - u_{i-1}(t^{n+1})|/u_{norm} \leq err_u$, $err_u \in \mathbb{R}^+$ and/or $|f_i(t^{n+1}) - f_{i-1}(t^{n+1})|/f_{norm} \leq err_f$, $err_f \in \mathbb{R}^+$
 - e) if criterion is satisfied time step is completed, else go to step a)
- 4) Dual-time step without fixed-point iteration.
 - i) Using the last estimate of the micro-scale apparent viscosity, compute flux corrections f_i

ii) Perform dual-time step update using n_{Newton} relaxation steps

if $n < N$ go to 1)

In the present dual-time step formulation, each fixed-point iteration corresponds to the solution of a 'pseudo-steady' problem using a Newton relaxation method, as discussed previously. For each increment of the fixed-point iteration counter, the micro-scale problem is marched forward by a pre-defined time-increment (in the present section, 10 Lennard-Jones time units) and the updated viscous flux correction will be checked with that at the previous iteration, while after the solution for the velocity field for iteration, also the convergence of the velocity field relative to the previous iteration is checked.

Table 1. Truncation criteria used in method 3

Criterion	$crit_{grad}$	err_u	err_f	fixed-point truncation
1A	0.05	0.25	0.25	or
1B	0.05	0.25	0.25	and
2A	0.05	0.50	0.50	or
2B	0.05	0.50	0.50	and

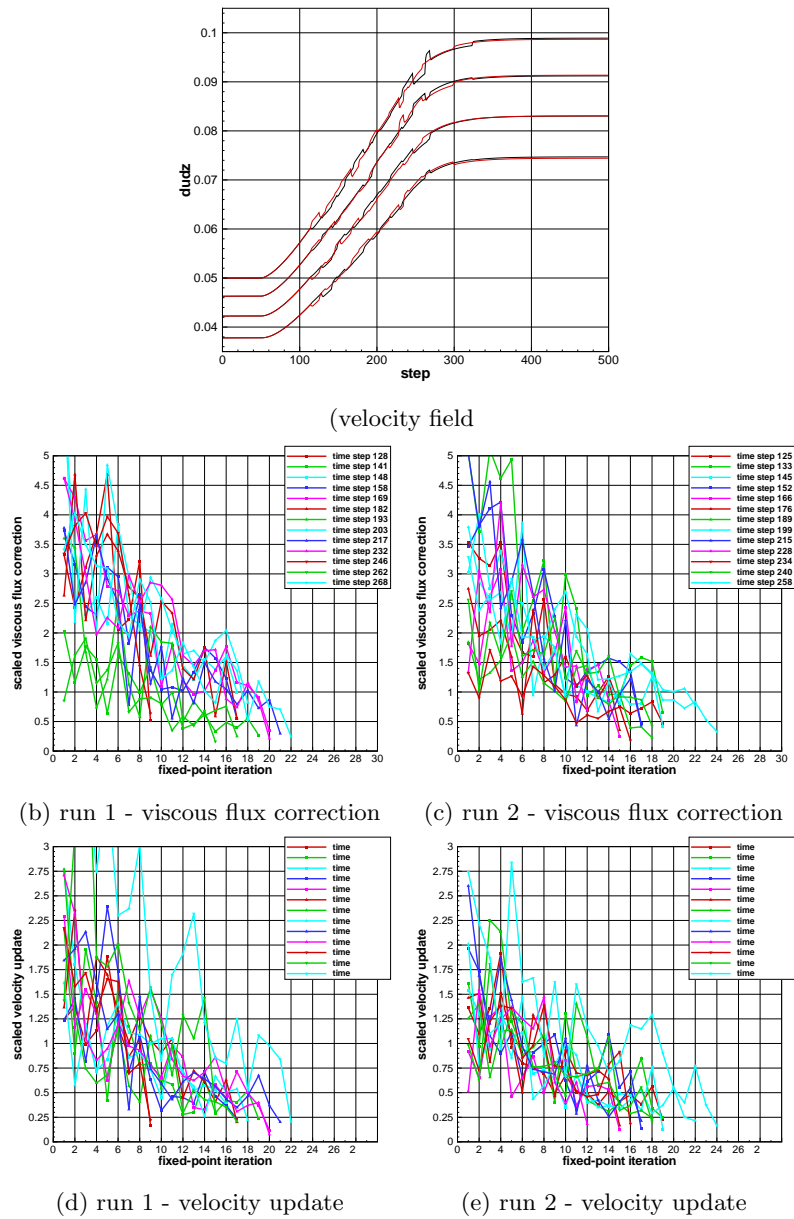


Fig. 8. Adaptive fixed-point scheme with truncation criteria 1A. Dual-time stepping method with adaptive MD sampling time in inner iterations. Finite-volume discretization with micro-scale viscous fluxes on first 4 cells near lower and upper walls. Approximate statistical scatter of Molecular Dynamics fluxes.

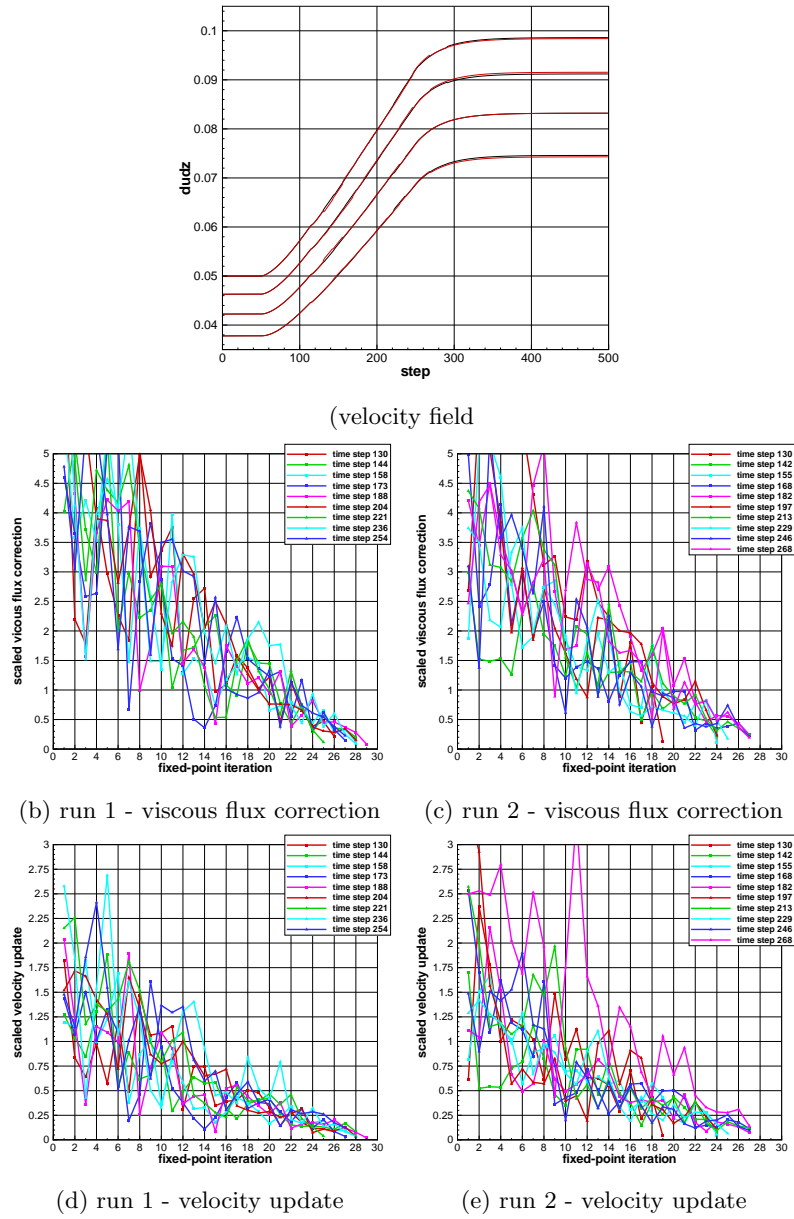


Fig. 9. Adaptive fixed-point scheme with truncation criteria 1B. Dual-time stepping method with adaptive MD sampling time in inner iterations. Finite-volume discretization with micro-scale viscous fluxes on first 4 cells near lower and upper walls. Approximate statistical scatter of Molecular Dynamics fluxes.

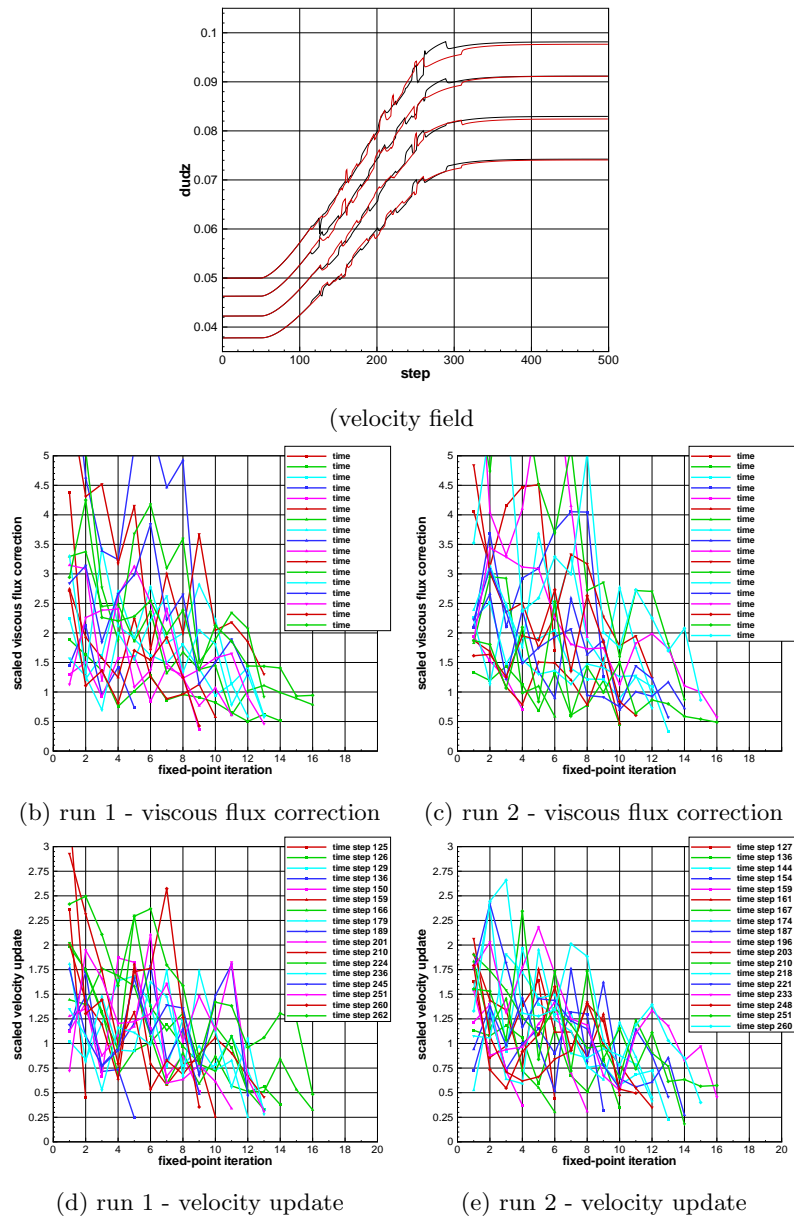
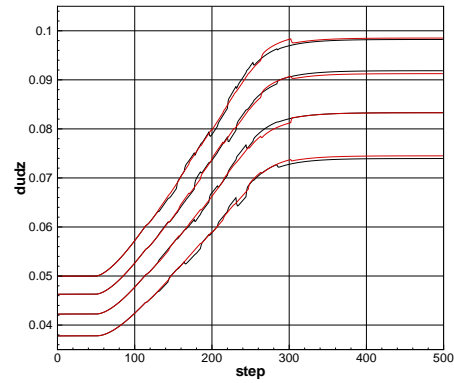
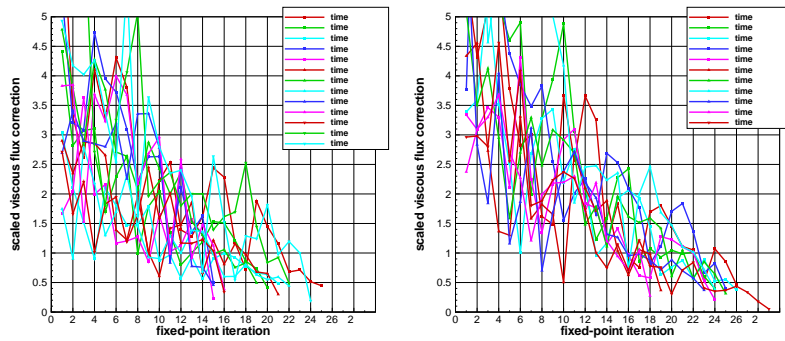


Fig. 10. Adaptive fixed-point scheme with truncation criteria 2A. Dual-time stepping method with adaptive MD sampling time in inner iterations. Finite-volume discretization with micro-scale viscous fluxes on first 4 cells near lower and upper walls. Approximate statistical scatter of Molecular Dynamics fluxes.

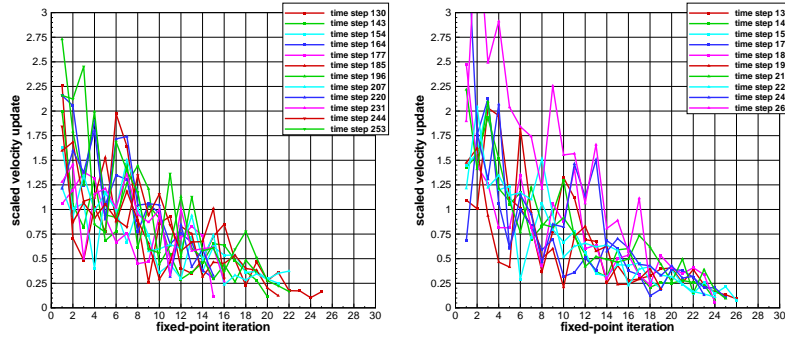


(a) velocity field



(c) run 1 - viscous flux correction

(d) run 2 - viscous flux correction



(e) run 1 - velocity update

(f) run 2 - velocity update

Fig. 11. Adaptive fixed-point scheme with truncation criteria 2B. Dual-time stepping method with adaptive MD sampling time in inner iterations. Finite-volume discretization with micro-scale viscous fluxes on first 4 cells near lower and upper walls. Approximate statistical scatter of Molecular Dynamics fluxes.

7 Conclusions and Discussions

We present an optimization of coupling Navier-Stokes and molecular Dynamics simulation by applying iterative operator-splitting methods. We discussed different techniques to reduce costly molecular dynamical computations by averaging, microscale models and adaptive iterations. Iterative and adaptive iterative splitting methods can reduce the costly coupling process and we obtain the same results as with costly computations. Here we have presented an accelerated solver with simultaneous coupling schemes. In future we will present more improved algorithms respecting multigrid schemes and nonlinear schemes. The analysis will be discussed in further papers.

References

1. M. Allen, D. Tildesly, *Computer Simulation of Liquids*, Clarendon Press, Oxford, 1987.
2. H. Berendsen, J. Postma, W. van Gunsteren, A. Dinola, J. Haak, *Molecular-Dynamics with Coupling to an External Bath*, *J. Chem. Phys.* 81 (1984) 3684–3690.
3. R.E. Ewing. Up-scaling of biological processes and multiphase flow in porous media. *IIMA Volumes in Mathematics and its Applications*, Springer-Verlag, 295 (2002), 195-215.
4. I. Farago, and Agnes Havasi. *On the convergence and local splitting error of different splitting schemes*. Eötvös Lorand University, Budapest, 2004.
5. P. Csomós, I. Faragó and A. Havasi. *Weighted sequential splittings and their analysis*. *Comput. Math. Appl.*, (to appear)
6. K.-J. Engel, R. Nagel, *One-Parameter Semigroups for Linear Evolution Equations*. Springer, New York, 2000.
7. I. Farago. *Splitting methods for abstract Cauchy problems*. *Lect. Notes Comp.Sci.* 3401, Springer Verlag, Berlin, 2005, pp. 35-45
8. I. Farago, J. Geiser. *Iterative Operator-Splitting methods for Linear Problems*. Preprint No. 1043 of the Weierstrass Institute for Applied Analysis and Stochastics, Berlin, Germany, June 2005.
9. P. Frolkovič and J. Geiser. *Numerical Simulation of Radionuclides Transport in Double Porosity Media with Sorption*. *Proceedings of Algorithmy 2000, Conference of Scientific Computing*, 28-36, 2000.
10. J. Geiser. *Numerical Simulation of a Model for Transport and Reaction of Radionuclides*. *Proceedings of the Large Scale Scientific Computations of Engineering and Environmental Problems*, Sozopol, Bulgaria, 2001.
11. J. Geiser. *Iterative Operator-Splitting Methods with higher order Time-Integration Methods and Applications for Parabolic Partial Differential Equations*. *Journal of Computational and Applied Mathematics*, Elsevier, Amsterdam, The Netherlands, 217, 227-242, 2008.
12. *Operator-Splitting Methods in Respect of Eigenvalue Problems for Nonlinear Equations and Applications to Burgers Equations*. *Journal of Computational and Applied Mathematics*, Elsevier, Amsterdam, accepted May 2009.
13. W. Hundsdorfer, L. Portero. *A Note on Iterated Splitting Schemes*. CWI Report MAS-E0404, Amsterdam, Netherlands, 2005.

14. W.H. Hundsdorfer, J. Verwer W. *Numerical solution of time-dependent advection-diffusion-reaction equations*, Springer, Berlin, (2003).
15. J. Irving, J. Kirkwood, The Statistical Mechanical Theory of Transport Processes IV, J. Chem. Phys. 18 (1950) 817–829.
16. J. Kanney, C. Miller and C. Kelley. *Convergence of iterative split-operator approaches for approximating nonlinear reactive transport problems*. Advances in Water Resources, 26:247–261, 2003.
17. P. van Leemput, W. Vanroose, and D. Roose. *Mesoscale analysis of the equation-free constrained runs initialization scheme* Multiscale Model. Simul. MODEL., 6(4), 1234–1255, 2008.
18. A. Lees, S. Edwards, The Computer Study of Transport Processes under Extreme Conditions, J. Phys. C 5 (1972) 1921–1929.
19. J. Lennard-Jones, Cohesion, Proc. Phys. Soc. 43 (1931) 461–482.
20. J. Van Lent. *Multigrid methods for time-dependent partial differential equations*. PhD Thesis, Katholieke Universiteit Leuven, Leuven, Belgium, 2006.
21. R.J. LeVeque. *Finite Volume Methods for Hyperbolic Problems*. Cambridge Texts in Applied Mathematics ,
22. G.I Marchuk. *Some applications of splitting-up methods to the solution of problems in mathematical physics*. Aplikace Matematiky, 1 (1968) 103-132.
23. R. Steijl and G.N. Barakos. Coupled Navier-Stokes - Molecular dynamics simulations using a multi-physics flow simulation framework. International Journal for Numerical Methods in Fluids, John Wiley, published online, 2009.
24. G. Strang. *On the construction and comparison of difference schemes*. SIAM J. Numer. Anal., 5:506–517, 1968.
25. L. Verlet, Computer Experiments of Classical Fluids. I. Thermodynamical Properties of Lennard-Jones Molecules, Physical Review 159 (1967) 98.
26. J.,G. Verwer and B. Sportisse. *A note on operator splitting in a stiff linear case*. MAS-R9830, ISSN 1386-3703, 1998.
27. S. Vandewalle. *Parallel Multigrid Waveform Relaxation for Parabolic Problems*. Teubner Skripten zur Numerik, B.G. Teubner Stuttgart, 1993.
28. Z. Zlatev. *Computer Treatment of Large Air Pollution Models*. Kluwer Academic Publishers, 1995.